PERGAMON

Engineering Fracture Mechanics 68 (2001) 403–416

Engineering Fracture Mechanics

www.elsevier.com/locate/engfracmech

Biaxial load effects on crack extension in anisotropic solids

Won-Kyun Lim [a,*], Seung-Yong Choi [a], Bhavani V. Sankar [b]

[a] *Department of Mechanical Engineering, Myongji University, Yongin, Kyonggi-do 449-728, South Korea*

[b] *Department of Aerospace Engineering, Mechanics and Engineering Science, University of Florida, Gainesville FL, Florida 32611, USA*

Received 21 February 2000; received in revised form 13 September 2000; accepted 2 October 2000

Abstract

The one-parameter singular expression for stresses and the corresponding displacements near a crack tip in anisotropic solids has been widely thought to be sufficiently accurate over a reasonable region for any geometry and loading conditions. In many cases, however subsequent terms of the series expansion are quantitatively significant, and hence we propose to consider the evaluation of such terms and their effect on the predicted crack growth direction. For this purpose the problem of horizontal-cracked orthotropic plate subjected to a biaxial loading is analyzed. It is assumed that the material is ideal homogeneous anisotropic. By considering the effect of the load applied parallel to the plane of the crack, the distribution of stresses and displacements at the crack tip is examined. In order to determine the direction of initial crack extension we employ the normal stress ratio criterion. The analysis is performed for a wide range of anisotropic material properties and applied loads. It is shown that the direction of crack extension can be seen to occur for nonzero values of θ_0 as the load parallel to the crack increases.

Keywords: Crack extension; Anisotropic solids; Biaxial loading; Nonsingular term

1. Introduction

Composites have found many applications as advanced engineering materials, effectively employed in various structural systems such as aircraft, automobiles, and power plants. The safety and reliability of these systems are dependent on the design of the constituent components. These components are often subjected to complex service loading conditions, in which two static principal stresses may exist. An advantage of using composites is the ability to tailor the stiffness and strength to specific design loads. Since most composite materials exhibit brittle failure with little or no ductility, as offered by metals, the behavior of the composite structure must be understood, and analysis to predict the failure needs to be performed.

A fundamental problem in predicting the failure of laminated composite materials is prediction of the direction of crack growth in the individual laminate as well as the laminate. Predicting the direction of crack extension in laminates is very complex three-dimensional problem. Since the lamina is the basic building block of the laminate, its behavior must be fully understood as a stepping stone toward

* Corresponding author. Fax: +82-31-321-4959.

E-mail address: limwk@wh.myongji.ac.kr (W.-K. Lim).

0013-7944/01/$ - see front matter
PII: S0013-7944(00)00103-X

understanding the behavior of the laminate. Thus, understanding the parameters that affect lamina failure, particularly those influencing the direction of crack growth in the lamina, is of critical importance in predicting the failure response of laminates.

The direction at which a fracture propagates in anisotropic material is a function of several variables. In anisotropic materials a variable material strength is associated with the potential direction of fracture. The crack direction is a function of the stress intensity factors, the crack orientation and the material strength. In designing against fracture in composite materials, especially fiber reinforced composite materials, the prediction of crack direction in anisotropic materials is of significance.

The general solution of the local stress and displacement fields in the vicinity of the crack in anisotropic bodies was obtained by Sih and Liebowitz [2] by using the Riemann–Hilbert formulation. In that analysis, they found an inverse square root stress singularity. When uniform load is applied on the surface of the crack, the nonsingular term related to outer boundary loading is omitted. Until recently the one-parameter singular expression for stress near a crack tip was widely thought to be sufficiently accurate over a reasonable region for any geometry and loading conditions [1–3].

In the present study, the problem of a cracked anisotropic plate subjected to a biaxial loading is analyzed. We consider the evaluation of the subsequent term of the series representation for the stresses and its effect on the predicted crack growth direction. It is assumed that the material is ideally homogeneous anisotropic. By considering the effect of the load applied parallel to the plane of the crack, the distribution of stresses and displacements at the crack tip is examined. In order to determine the direction of initial crack extension we employ the normal stress ratio theory [4]. Our goal here is to show that the angle of crack extension can be altered by loads applied parallel to a crack and the use of second order term in the series expansion is essential for the accurate determination of crack growth direction.

2. Fundamental equations in homogeneous anisotropic solids

A plate of homogeneous rectilinearly anisotropic material whose principal axes of material symmetry coincide with the x and y directions is considered. The stress–strain relationship for the two-dimensional case can be written in terms of compliance coefficients as

$$\begin{pmatrix} \varepsilon_{xx} \\ \varepsilon_{yy} \\ \gamma_{xy} \end{pmatrix} = \begin{bmatrix} a_{11} & a_{12} & a_{16} \\ a_{12} & a_{22} & a_{26} \\ a_{16} & a_{26} & a_{66} \end{bmatrix} \begin{pmatrix} \sigma_{xx} \\ \sigma_{yy} \\ \tau_{xy} \end{pmatrix} \tag{1}$$

where a_{ij} $(i,j = 1,2,6)$ are the compliance coefficients.

The compatibility equation can be represented in terms of Airy's stress function, $U(x,y)$ as

$$a_{22}\frac{\partial^4 U}{\partial x^4} - 2a_{26}\frac{\partial^4 U}{\partial x^3\,\partial y} + (2a_{12} + a_{66})\frac{\partial^4 U}{\partial x^2\,\partial y^2} - 2a_{16}\frac{\partial^4 U}{\partial x\,\partial y^3} + a_{11}\frac{\partial^4 U}{\partial y^4} = 0 \tag{2}$$

The general expression of Eq. (2) in plane elasticity problem can be written in terms of complex variables as [5]

$$U(x,y) = 2\mathrm{Re}[U_1(z_1) + U_2(z_2)] \tag{3}$$

where Re indicates the real part of the complex, $U_1(z_1)$ and $U_2(z_2)$ are stress function of complex variables $z_1 = x + s_1 y$ and $z_2 = x + s_2 y$, and s_1 and s_2 are roots of the following characteristic equation:

$$a_{11}s^4 - 2a_{16}s^3 + (2a_{12} + a_{66})s^2 - 2a_{26}s + a_{22} = 0 \tag{4}$$

To simplify Eq. (3), we introduce new functions, $\phi(z_1)$ and $\psi(z_2)$. Then, the stress and displacement components can be expressed as

$$\begin{aligned}\sigma_{xx} &= 2\,\mathrm{Re}[s_1^2\phi'(z_1) + s_2^2\psi'(z_2)]\\ \sigma_{yy} &= 2\,\mathrm{Re}[\phi'(z_1) + \psi'(z_2)]\\ \tau_{xy} &= -2\,\mathrm{Re}[s_1\phi'(z_1) + s_2\psi'(z_2)]\end{aligned} \tag{5}$$

$$\begin{aligned}u(x,y) &= 2\,\mathrm{Re}[p_1\phi(z_1) + p_2\psi(z_2)]\\ v(x,y) &= 2\,\mathrm{Re}[q_1\phi(z_1) + q_2\psi(z_2)]\end{aligned} \tag{6}$$

where $\phi'(z_1) = \mathrm{d}\phi(z_1)/\mathrm{d}z_1$ and $\psi'(z_2) = \mathrm{d}\psi(z_2)/\mathrm{d}z_2$. p_j and q_j $(j = 1, 2)$ are given as

$$\begin{aligned}p_1 &= a_{11}s_1^2 + a_{12} - a_{16}s_1, \qquad p_2 = a_{11}s_2^2 + a_{12} - a_{16}s_2,\\ q_1 &= \frac{a_{12}s_1^2 + a_{22} - a_{26}s_1}{s_1}, \qquad q_2 = \frac{a_{12}s_2^2 + a_{22} - a_{26}s_2}{s_2},\end{aligned} \tag{7}$$

In orthotropic solids of elastic symmetry, $a_{16} = a_{26} = 0$ and the characteristic equation of Eq. (4) can be simplified as

$$a_{11}s^4 + (2a_{12} + a_{66})s^2 + a_{22} = 0 \tag{8}$$

Then, the roots of the characteristic equation is given as

$$\begin{aligned}s_1 &= \sqrt{\frac{\alpha_0 - \beta_0}{2}} + \mathrm{i}\sqrt{\frac{\alpha_0 + \beta_0}{2}} = \alpha_1 + \mathrm{i}\beta_1\\ s_2 &= \sqrt{\frac{\alpha_0 - \beta_0}{2}} + \mathrm{i}\sqrt{\frac{\alpha_0 + \beta_0}{2}} = \alpha_2 + \mathrm{i}\beta_2\end{aligned} \tag{9}$$

where

$$\alpha_0 = \sqrt{\frac{a_{22}}{a_{11}}} = \sqrt{\frac{E_{11}}{E_{22}}} \quad \text{and} \quad \beta_0 = \frac{1}{a_{11}}\left(\frac{a_{66}}{2} + a_{12}\right) = \frac{E_{11}}{2\mu_{12}} - \nu_{12} : \alpha_0 > \beta_0$$

3. Analytic functions for a horizontal-crack in infinite anisotropic plate under biaxial loading

In order to derive the analytic function ϕ and ψ including the nonsingular term in anisotropic cracked problem under biaxial loading, we consider an elliptical hole in an infinite plate under tension as shown in Fig. 1. When an elliptical hole in a plate is subjected to uniaxial stress at an angle α with the x-axis, the analytic function is given as follows by Savin [6]

$$\begin{aligned}\phi^{(\alpha)}(z_1) &= \phi_0^{(\alpha)}(z_1) + B^{*(\alpha)}z_1\\ \psi^{(\alpha)}(z_2) &= \psi_0^{(\alpha)}(z_2) + [B'^{*(\alpha)} + \mathrm{i}C'^{*(\alpha)}]z_2\end{aligned} \tag{10}$$

where $\phi_0^{(\alpha)}(z_1)$, $\psi_0^{(\alpha)}(z_2)$, $B^{*(\alpha)}$, $B'^{*(\alpha)}$, and $C'^{*(\alpha)}$ are defined as

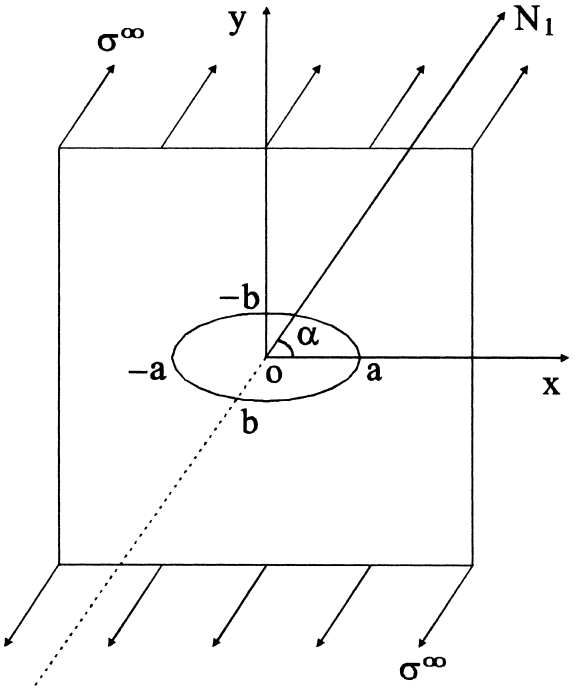

Fig. 1. Anisotropic plate with an elliptical hole under tension.

$$\phi_0^{(\alpha)}(z_1) = -\frac{i\sigma^\infty(a - is_1 b)}{4(s_1 - s_2)}\left\{\frac{b(s_2\sin 2\alpha + 2\cos^2\alpha)}{z_1 + \sqrt{z_1^2 - (a^2 + s_1^2 b^2)}} + \frac{ia(2s_2\sin^2\alpha + \sin 2\alpha)}{z_1 + \sqrt{z_1^2 - (a^2 + s_1^2 b^2)}}\right\}$$

$$\psi_0^{(\alpha)}(z_2) = \frac{i\sigma^\infty(a - is_2 b)}{4(s_1 - s_2)}\left\{\frac{b(s_1\sin 2\alpha + 2\cos^2\alpha)}{z_2 + \sqrt{z_2^2 - (a^2 + s_2^2 b^2)}} + \frac{ia(2s_1\sin^2\alpha + \sin 2\alpha)}{z_2 + \sqrt{z_2^2 - (a^2 + s_2^2 b^2)}}\right\}$$

$$B^{*(\alpha)} = \sigma^\infty \frac{\cos^2\alpha + (\alpha_2^2 + \beta_2^2)\sin^2\alpha + \alpha_2\sin 2\alpha}{2[(\alpha_2 - \alpha_1)^2 + (\beta_2^2 - \beta_1^2)]} \tag{11}$$

$$B'^{*(\alpha)} = \sigma^\infty \frac{[(\alpha_1^2 - \beta_1^2) - 2\alpha_1\alpha_2]\sin^2\alpha - \cos^2\alpha - \alpha_2\sin 2\alpha}{2[(\alpha_2 - \alpha_1)^2 + (\beta_2^2 - \beta_1^2)]}$$

$$C'^{*(\alpha)} = \sigma^\infty\left\{\frac{(\alpha_1 - \alpha_2)\cos^2\alpha + [\alpha_2(\alpha_1^2 - \beta_1^2) - \alpha_1(\alpha_2^2 - \beta_2^2)]\sin^2\alpha}{2\beta_2[(\alpha_2 - \alpha_1)^2 + (\beta_2^2 - \beta_1^2)]} + \frac{[(\alpha_1^2 - \beta_1^2) - (\alpha_2^2 - \beta_2^2)]\sin\alpha\cos\alpha}{2\beta_2[(\alpha_2 - \alpha_1)^2 + (\beta_2^2 - \beta_1^2)]}\right\}$$

Therefore if α equals $\pi/2$, the analytic function can be represented as

$$\phi^{(\alpha=\pi/2)}(z_1) = \phi_0^{(\alpha=\pi/2)}(z_1) + B^{*(\alpha=\pi/2)}z_1$$
$$\psi^{(\alpha=\pi/2)}(z_2) = \psi_0^{(\alpha=\pi/2)}(z_2) + [B'^{*(\alpha=\pi/2)} + iC'^{*(\alpha=\pi/2)}]z_2 \tag{12}$$

where $\phi_0^{(\alpha=\pi/2)}(z_1)$, $\psi_0^{(\alpha=\pi/2)}(z_2)$, $B^{*(\alpha=\pi/2)}$, $B'^{*(\alpha=\pi/2)}$ and $C'^{*(\alpha=\pi/2)}$ are defined as

$$\begin{aligned}
\phi_0^{(\alpha=\pi/2)}(z_1) &= -\frac{\mathrm{i}\sigma^\infty(a-\mathrm{i}s_1 b)}{4(s_1-s_2)}\left\{\frac{\mathrm{i}2as_2}{z_1+\sqrt{z_1^2-(a^2+s_1^2b^2)}}\right\}\\
\psi_0^{(\alpha=\pi/2)}(z_2) &= \frac{\mathrm{i}\sigma^\infty(a-\mathrm{i}s_2 b)}{4(s_1-s_2)}\left\{\frac{\mathrm{i}2as_1}{z_2+\sqrt{z_2^2-(a^2+s_2^2b^2)}}\right\}\\
B^{*(\alpha=\pi/2)} &= \frac{\sigma^\infty(\alpha_2^2+\beta_2^2)}{2[(\alpha_2-\alpha_1)^2+(\beta_2^2-\beta_1^2)]}\\
B'^{*(\alpha=\pi/2)} &= \frac{\sigma^\infty[(\alpha_1^2-\beta_1^2)-2\alpha_1\alpha_2]}{2[(\alpha_2-\alpha_1)^2+(\beta_2^2-\beta_1^2)]}\\
C'^{*(\alpha=\pi/2)} &= \frac{\sigma^\infty[\alpha_2(\alpha_1^2-\beta_1^2)-\alpha_1(\alpha_2^2-\beta_2^2)]}{2\beta_2[(\alpha_2-\alpha_1)^2+(\beta_2^2-\beta_1^2)]}
\end{aligned} \tag{13}$$

The analytic function in the case of $\alpha = 0$ is determined similarly from Eq. (10) and is given as

$$\begin{aligned}
\phi^{(\alpha=0)}(z_1) &= \phi_0^{(\alpha=0)}(z_1) + B^{*(\alpha=0)}z_1\\
\psi^{(\alpha=0)}(z_2) &= \psi_0^{(\alpha=0)}(z_2) + [B'^{*(\alpha=0)} + \mathrm{i}C'^{*(\alpha=0)}]z_2
\end{aligned} \tag{14}$$

where $\phi_0^{(\alpha=0)}(z_1)$, $\psi_0^{(\alpha=0)}(z_2)$, $B^{*(\alpha=0)}$, $B'^{*(\alpha=0)}$ and $C'^{*(\alpha=0)}$ are defined as

$$\begin{aligned}
\phi_0^{(\alpha=0)}(z_1) &= -\frac{\mathrm{i}k\sigma^\infty(a-\mathrm{i}s_1 b)}{4(s_1-s_2)}\left\{\frac{2b}{z_1+\sqrt{z_1^2-(a^2+s_1^2b^2)}}\right\}\\
\psi_0^{(\alpha=0)}(z_2) &= \frac{\mathrm{i}k\sigma^\infty(a-\mathrm{i}s_2 b)}{4(s_1-s_2)}\left\{\frac{-2b}{z_2+\sqrt{z_2^2-(a^2+s_2^2b^2)}}\right\}\\
B^{*(\alpha=0)} &= \frac{k\sigma^\infty}{2[(\alpha_2-\alpha_1)^2+(\beta_2^2-\beta_1^2)]}\\
B'^{*(\alpha=0)} &= \frac{-k\sigma^\infty}{2[(\alpha_2-\alpha_1)^2+(\beta_2^2-\beta_1^2)]}\\
C'^{*(\alpha=0)} &= \frac{k\sigma^\infty(\alpha_1-\alpha_2)}{2\beta_2[(\alpha_2-\alpha_1)^2+(\beta_2^2-\beta_1^2)]}
\end{aligned} \tag{15}$$

Thus, the analytic functions for a horizontal-crack under biaxial loading as shown in Fig. 2 can be derived by combining the functions given in Eqs. (12) and (14), and substituting zero for the short radius of elliptical hole, i.e., $b = 0$. The analytic function on crack tip can be expressed as

$$\begin{aligned}
\phi(z_1) &= \frac{\sigma^\infty s_2}{2(s_1-s_2)}\left[z_1-\sqrt{z_1^2-a^2}\right] + \Gamma_1 z_1\\
\psi(z_2) &= -\frac{\sigma^\infty s_1}{2(s_1-s_2)}\left[z_2-\sqrt{z_2^2-a^2}\right] + \Gamma_2 z_2
\end{aligned} \tag{16}$$

where $\Gamma_1 = B^*$ and $\Gamma_2 = (B'^* + \mathrm{i}C'^*)$. B^*, B'^* and C'^* are real constants computed from material properties and external loads as

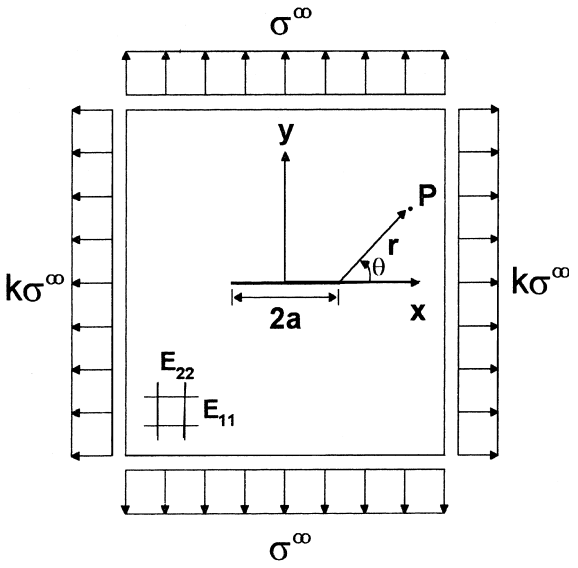

Fig. 2. Plane biaxially loaded center-crack geometry.

$$
\begin{aligned}
B^{*} &= \frac{k\sigma^{\infty} + (\alpha_2^2 + \beta_2^2)\sigma^{\infty}}{2[(\alpha_2 - \alpha_1)^2 + (\beta_2^2 - \beta_1^2)]} \\
B'^{*} &= \frac{[(\alpha_1^2 - \beta_1^2) - 2\alpha_1\alpha_2]\sigma^{\infty} - k\sigma^{\infty}}{2[(\alpha_2 - \alpha_1)^2 + (\beta_2^2 - \beta_1^2)]} \\
C'^{*} &= \left\{ \frac{(\alpha_1 - \alpha_2)k\sigma^{\infty} + [\alpha_2(\alpha_1^2 - \beta_1^2) - \alpha_1(\alpha_2^2 - \beta_2^2)]\sigma^{\infty}}{2\beta_2[(\alpha_2 - \alpha_1)^2 + (\beta_2^2 - \beta_1^2)]} \right\}
\end{aligned}
\tag{17}
$$

4. Stress and displacement components including nonsingular term

Calculation may be facilitated by use of coordinate ζ_j originating at the crack tip.

$$z_j - a = \zeta_j = r(\cos\theta + s_j \sin\theta), \quad z_j = x + s_j y$$

Thus, the analytic function of Eq. (16) and its first order derivative are given as

$$
\begin{aligned}
\phi(\zeta_1) &= \frac{\sigma^{\infty} s_2}{2(s_1 - s_2)} \left[(\zeta_1 + a) - \sqrt{\zeta_1^2 + 2a\zeta_1} \right] + \Gamma_1(\zeta_1 + a) \\
\psi(\zeta_2) &= -\frac{\sigma^{\infty} s_1}{2(s_1 - s_2)} \left[(\zeta_2 + a) - \sqrt{\zeta_2^2 + 2a\zeta_2} \right] + \Gamma_2(\zeta_2 + a) \\
\phi'(\zeta_1) &= \frac{\sigma^{\infty} s_2}{2(s_1 - s_2)} \left[1 - \frac{\zeta_1 + a}{\sqrt{\zeta_1^2 + 2a\zeta_1}} \right] + \Gamma_1 \\
\psi'(\zeta_2) &= -\frac{\sigma^{\infty} s_1}{2(s_1 - s_2)} \left[1 - \frac{\zeta_2 + a}{\sqrt{\zeta_2^2 + 2a\zeta_2}} \right] + \Gamma_2
\end{aligned}
\tag{18}
$$

Expressing the right sides of $\phi'(\zeta_1)$ and $\psi'(\zeta_2)$ in Eq. (18) as power series expansion, the above equation can be expressed as

$$\begin{aligned}\phi'(\zeta_1) &= -\frac{\sigma^\infty s_2}{2(s_1-s_2)}\left\{\frac{1}{\sqrt{2}}\left[\left(\frac{\zeta_1}{a}\right)^{-\frac{1}{2}}+\frac{3}{4}\left(\frac{\zeta_1}{a}\right)^{\frac{1}{2}}-\frac{5}{32}\left(\frac{\zeta_1}{a}\right)^{\frac{3}{2}}+\cdots\right]\right\}+\frac{\sigma^\infty s_2}{2(s_1-s_2)}+\Gamma_1\\ \psi'(\zeta_2) &= \frac{\sigma^\infty s_1}{2(s_1-s_2)}\left\{\frac{1}{\sqrt{2}}\left[\left(\frac{\zeta_2}{a}\right)^{-\frac{1}{2}}+\frac{3}{4}\left(\frac{\zeta_2}{a}\right)^{\frac{1}{2}}-\frac{5}{32}\left(\frac{\zeta_2}{a}\right)^{\frac{3}{2}}+\cdots\right]\right\}-\frac{\sigma^\infty s_1}{2(s_1-s_2)}+\Gamma_2\end{aligned} \tag{19}$$

Ignoring the higher order terms of ζ_1 and ζ_2, $\phi'(\zeta_1)$ and $\psi'(\zeta_2)$ can be simplified as

$$\begin{aligned}\phi'(\zeta_1) &\cong -\frac{\sigma^\infty s_2}{2\sqrt{2}(s_1-s_2)}\left[\left(\frac{\zeta_1}{a}\right)^{-\frac{1}{2}}\right]+\frac{\sigma^\infty s_2}{2(s_1-s_2)}+\Gamma_1\\ \psi'(\zeta_2) &\cong \frac{\sigma^\infty s_1}{2\sqrt{2}(s_1-s_2)}\left[\left(\frac{\zeta_2}{a}\right)^{-\frac{1}{2}}\right]-\frac{\sigma^\infty s_1}{2(s_1-s_2)}+\Gamma_2\end{aligned} \tag{20}$$

Thus, by substituting $\phi'(\zeta_1)$ and $\psi'(\zeta_2)$ into Eq. (5), the crack tip stresses including the nonsingular term can be expressed as

$$\begin{aligned}\sigma_{xx} &= \frac{K_{\mathrm{I}}}{\sqrt{2\pi r}}\mathrm{Re}\left[\frac{s_1 s_2}{(s_1-s_2)}\left(\frac{s_2}{\sqrt{\cos\theta+s_2\sin\theta}}-\frac{s_1}{\sqrt{\cos\theta+s_1\sin\theta}}\right)\right]+\sigma^\infty\mathrm{Re}[s_1 s_2+k]\\ \sigma_{yy} &= \frac{K_{\mathrm{I}}}{\sqrt{2\pi r}}\mathrm{Re}\left[\frac{1}{(s_1-s_2)}\left(\frac{s_1}{\sqrt{\cos\theta+s_2\sin\theta}}-\frac{s_2}{\sqrt{\cos\theta+s_1\sin\theta}}\right)\right]\\ \tau_{xy} &= \frac{K_{\mathrm{I}}}{\sqrt{2\pi r}}\mathrm{Re}\left[\frac{s_1 s_2}{(s_1-s_2)}\left(\frac{1}{\sqrt{\cos\theta+s_1\sin\theta}}-\frac{1}{\sqrt{\cos\theta+s_2\sin\theta}}\right)\right]\end{aligned} \tag{21}$$

where $K_{\mathrm{I}}=\sigma^\infty\sqrt{\pi a}$.

Similarly, in order to derive displacement components near a crack tip it is necessary to express the right sides of $\phi(\zeta_1)$ and $\psi(\zeta_2)$ in Eq. (18) as power series expansion. Ignoring the higher order terms of ζ_1 and ζ_2, $\phi(\zeta_1)$ and $\psi(\zeta_2)$ can be simplified as

$$\begin{aligned}\phi(\zeta_1) &\cong \frac{\sigma^\infty s_2}{2(s_1-s_2)}\left[(\zeta_1+a)-\sqrt{2\zeta_1 a}\right]+\Gamma_1(\zeta_1+a)\\ \psi(\zeta_2) &\cong -\frac{\sigma^\infty s_1}{2(s_1-s_2)}\left[(\zeta_2+a)-\sqrt{2\zeta_2 a}\right]+\Gamma_2(\zeta_2+a)\end{aligned} \tag{22}$$

Thus, by substituting the above equation into Eq. (6), the crack tip displacements can be expressed as

$$\begin{aligned}u(x,y) &= K_{\mathrm{I}}\sqrt{\frac{2r}{\pi}}\mathrm{Re}\left[\frac{1}{(s_1-s_2)}\left(s_1 p_2\sqrt{\cos\theta+s_2\sin\theta}-s_2 p_1\sqrt{\cos\theta+s_1\sin\theta}\right)\right]+\sigma^\infty\mathrm{Re}\left[\frac{s_2 p_1-s_1 p_2}{s_1-s_2}\right]\\ &\quad\times(r\cos\theta+a)+\sigma^\infty\mathrm{Re}\left[\frac{p_1-p_2}{s_1-s_2}s_1 s_2\right](r\sin\theta)+2\mathrm{Re}[p_1\Gamma_1+p_2\Gamma_2](r\cos\theta+a)+2\mathrm{Re}[s_1 p_1\Gamma_1\\ &\quad+s_2 p_2\Gamma_2](r\sin\theta)\\ v(x,y) &= K_{\mathrm{I}}\sqrt{\frac{2r}{\pi}}\mathrm{Re}\left[\frac{1}{(s_1-s_2)}\left(s_1 q_2\sqrt{\cos\theta+s_2\sin\theta}-s_2 q_1\sqrt{\cos\theta+s_1\sin\theta}\right)\right]\\ &\quad+\sigma^\infty\mathrm{Re}\left[\frac{s_2 q_1-s_1 q_2}{s_1-s_2}\right](r\cos\theta+a)+\sigma^\infty\mathrm{Re}\left[\frac{q_1-q_2}{s_1-s_2}s_1 s_2\right](r\sin\theta)+2\mathrm{Re}[q_1\Gamma_1+q_2\Gamma_2]\\ &\quad\times(r\cos\theta+a)+2\mathrm{Re}[s_1 q_1\Gamma_1+s_2 q_2\Gamma_2](r\sin\theta)\end{aligned} \tag{23}$$

In this case, we observe from Eqs. (21) and (23) that second order term makes significant contribution. In particular we note that the effects of the horizontal load appear only in the secondary terms. Thus, far from being negligible second order terms, they have an important influence on results obtained.

5. Direction of initial crack extension

In order to show the effects of the loads parallel to the plane of the crack on the predicted crack growth direction we employ the normal stress ratio theory. This criterion, proposed by Buczek and Herakovich [4], is a direct extension of the maximum circumferential tensile stress criterion, formulated to make it applicable to anisotropic fracture problems. The model assumes that a direction of crack extension is determined by the ratio of normal stress acting on a radial plane, $\sigma_{\theta\theta}$, to the related strength, $T_{\theta\theta}$. Crack extension will take place in the direction in which the ratio at a given distance, r_0 $(0 < r_0 \ll 1)$, from the crack tip, R_0, is of maximum value. Here, R_0 is defined as

$$R_0(r_0,\theta) = \frac{\sigma_{\theta\theta}(r_0,\theta)}{T_{\theta\theta}} \tag{24}$$

where $T_{\theta\theta}$ is the tensile strength on the θ plane and is defined as

$$T_{\theta\theta} = X_T \sin^2\theta + Y_T \cos^2\theta \tag{25}$$

In the above expression X_T and Y_T are the tensile strengths in anisotropic solids to longitudinal and transverse directions, respectively and $\sigma_{\theta\theta}$ is the normal stress which can be calculated from

$$\sigma_{\theta\theta} = \sigma_{xx}\sin^2\theta + \sigma_{yy}\cos^2\theta - 2\tau_{xy}\sin\theta\cos\theta \tag{26}$$

Substituting the rectangular stress components of Eq. (21) into Eq. (26) the normal stress including non-singular term can be expressed as

$$\sigma_{\theta\theta} = \frac{\sigma^\infty}{\sqrt{2}}\sqrt{\frac{a}{r}}\,\mathrm{Re}\left[\frac{1}{(s_1-s_2)}\left[s_1(\cos\theta + s_2\sin\theta)^{3/2} - s_2(\cos\theta + s_1\sin\theta)^{3/2}\right]\right] + \sigma^\infty \mathrm{Re}[s_1 s_2 + k]\sin^2\theta \tag{27}$$

Thus algorithmically, the direction of crack extension θ_0 is found by maximizing Eq. (24) or its normalized equivalent as

$$\mathrm{Max}\left(\frac{\left[\frac{1}{\sqrt{2}}\sqrt{\frac{a}{r}}\,\mathrm{Re}\left[\frac{1}{(s_1-s_2)}\left[s_1(\cos\theta + s_2\sin\theta)^{3/2} - s_2(\cos\theta + s_1\sin\theta)^{3/2}\right]\right] + \mathrm{Re}[s_1 s_2 + k]\sin^2\theta\right]}{\sin^2\theta + \frac{Y_T}{X_T}\cos^2\theta}\right) \tag{28}$$

6. Results and discussion

We now turn to the familiar cracked sheet problem with biaxially loaded boundary conditions as shown in Fig. 2. To investigate the effects of biaxial loading more clearly, we analyze the distribution of the circumferential stress near crack tip. Fig. 3 shows the variation of normalized circumferential stress, $\sigma_{\theta\theta}/\sigma^\infty$ with polar angle, θ plotted for different values of horizontal ratio, k with $\alpha_0 = 3.0$ and $\beta_0 = 1.0$. The curves were obtained with the ratio, r_0/a taken to be 0.01, which is arbitrary since r_0/a is left unspecified. As shown in figure, the positive maximum of circumferential stresses can be seen to occur for nonzero value of θ,

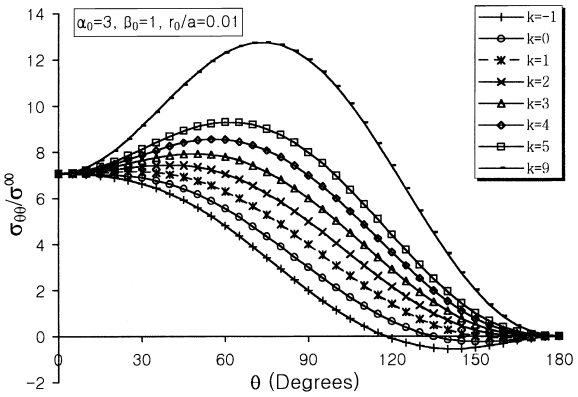

Fig. 3. Variation of $\sigma_{\theta\theta}$ with k for $\alpha_0 = 3$ and $\beta_0 = 1$.

which increases as k increases, starting in the vicinity of $k = 0$. This graph further indicates that the effects of k on the distribution of the circumferential stress are particularly represented as k has high values. Our analysis demonstrates quite conclusively the importance of the nonsingular term to expression (27).

In order to examine further the effects of biaxial loading we predict the direction of initial crack extension for the biaxially loaded sheet with a horizontal crack. As noted previously, the point of crack initiation is selected on the basis of maximum value of the normal stress ratio, R acting on crack boundary. The direction of crack extension is measured from a direction parallel to the x-axis passing through this point of crack initiation.

We calculated R–θ curves for the three cases of the tensile strength ratio, Y_T/X_T being equal to $1/1.5$, $1/2$ and $1/3$ with $\alpha_0 = 2.0$ and $\beta_0 = 1.0$. The results based on the case $r_0/a = 0.01$ are shown in Figs. 4–6. At first, Fig. 4 shows the results for the case of $Y_T/X_T = 1/1.5$. As shown in figure, the maximum normal stress ratio takes place along the plane of the original crack for uniaxial load. So the direction of the crack extension occurs at $\theta_0 = 0$. However, in the case of biaxial load the maximum normal stress ratio can be seen to occur for nonzero value of θ_0 although the crack shape and the applied load are symmetric. The crack extension therefore begins to turn from the value of $\theta_0 = 0$. It is starting in the vicinity of $k = 6$ and

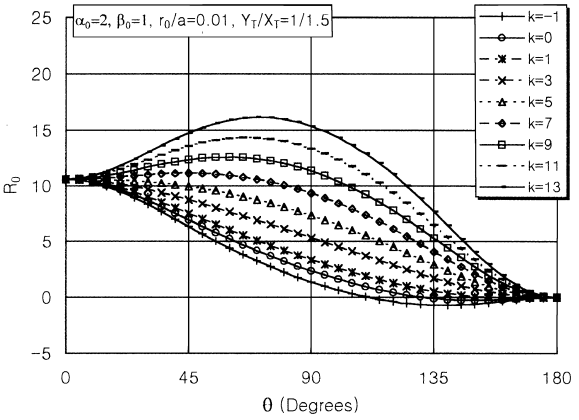

Fig. 4. Variation of R_0 with k for $\alpha_0 = 2$, $\beta_0 = 1$ and $Y_T/X_T = 1/1.5$.

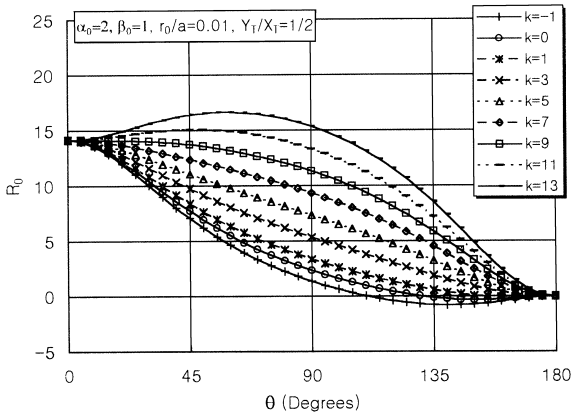

Fig. 5. Variation of R_0 with k for $\alpha_0 = 2$, $\beta_0 = 1$ and $Y_T/X_T = 1/2$.

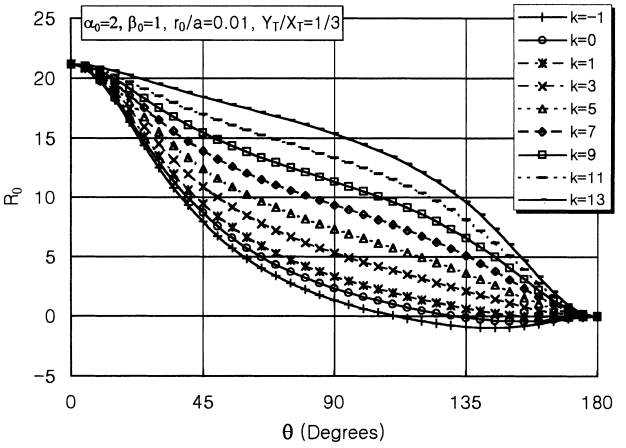

Fig. 6. Variation of R_0 with k for $\alpha_0 = 2$, $\beta_0 = 1$ and $Y_T/X_T = 1/3$.

increases as k increases. For example, the predicted direction of initial crack extension is $\theta_0 = 44.6°$ for k having a value of 7 and $\theta_0 = 66.3°$ for k having a value of 11. As the horizontal tension becomes large relative to the vertical tension the direction of initial crack extension turns so as to be oriented normal to the direction of the larger of the tensile loads. Fig. 5 shows the results for the case of $Y_T/X_T = 1/2$. For values of k greater than 9 the maximum normal stress ratio can be seen to occur for nonzero value of θ_0. So the crack extension deviates from the plane of the original crack. It can be seen that the effects of horizontal load ratio to the direction of crack extension decrease as the difference of the tensile strengths increases. We can see the phenomenon more clearly in the case of $Y_T/X_T = 1/3$ shown in Fig. 6. The maximum normal stress ratio can be seen to occur for zero value of θ_0 in the case $k = 13$ though. If a value of k greater than 13 is applied the crack extension will gradually deviate from the plane of the original crack. The predicted directions of initial crack extension are compared in Table 1 for various horizontal load ratio and two r_0/a ratios. The predicted propagation direction becomes very much dependent on the ratio r_0/a, especially for large values of $Y_T/X_T = 1/1.5$ (see Table 1). The critical value of r_0/a for a given material should be determined by performing experiments.

Table 1
Predicted direction of initial crack extension for various horizontal load ratio with $\alpha_0 = 2.0$ and $\beta_0 = 1.0$

k	θ_0 (degrees)					
	$Y_T/X_T = 1/1.5$		$Y_T/X_T = 1/2$		$Y_T/X_T = 1/3$	
	$r_0/a = 0.01$	0.05	$r_0/a = 0.01$	0.05	$r_0/a = 0.01$	0.05
−1	0	0	0	0	0	0
1	0	0	0	0	0	0
2	0	0	0	0	0	0
3	0	0	0	0	0	0
4	0	±37.9	0	0	0	0
5	0	±57.5	0	0	0	0
6	±28.9	±66.2	0	±46.5	0	0
7	±44.6	±71.2	0	±58.9	0	0
8	±53.2	±74.5	0	±65.6	0	0
9	±59.0	±76.8	0	±69.8	0	±40.7
10	±63.2	±78.5	±36.6	±72.8	0	±53.4
11	±66.3	±79.8	±47.0	±75.0	0	±60.3
12	±68.9	±80.9	±53.5	±76.7	0	±64.8
13	±70.9	±81.7	±58.2	±78.1	0	±68.1

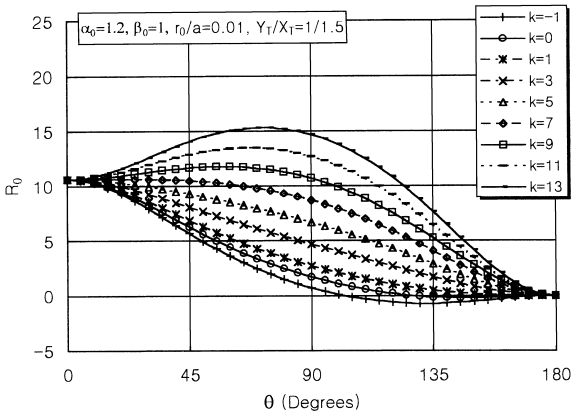

Fig. 7. Variation of R_0 with k for $\alpha_0 = 1.2$, $\beta_0 = 1$ and $Y_T/X_T = 1/1.5$.

Next calculated R–θ curves for three cases of the elastic modulus ratio, α_0 being equal to 1.2, 3.0 and 5.0 with $Y_T/X_T = 1/1.5$ and $\beta_0 = 1.0$. The results based on the case of $r_0/a = 0.01$ are shown in Figs. 7–9. In the figures we note that the value of the horizontal load ratio to deviate the crack extension from the plane of the original crack decreases as the elastic modulus ratio increases. For example, the maximum normal stress ratio takes a nonzero value of θ_0 around $k = 7$ in the case of $\alpha_0 = 1.2$, $k = 4$ in $\alpha_0 = 3.0$ and $k = 1$ in $\alpha_0 = 5.0$. It can be seen that the effects of the horizontal load ratio on the predicted direction of crack extension generally increase as the material becomes more anisotropic. However, in the case of $r_0/a = 0.05$ the value of the horizontal load ratio to deviate the crack extension occurs in about 4 for all three α_0 ratios as shown in Table 2.

As a further example, we examined the crack extension for horizontal crack under uniaxial tension load. We calculated R–θ curves for the four cases of the elastic modulus ratio α_0 being equal to 1.2, 2.0, 3.0, and 5.0 with $\beta_0 = 1.0$ and $Y_T/X_T = 1/1.5$. The results in Fig. 10 are computed by taking singular term only, and results in Fig. 11 are based on the appropriate value of nonsingular term. A comparison between predicted

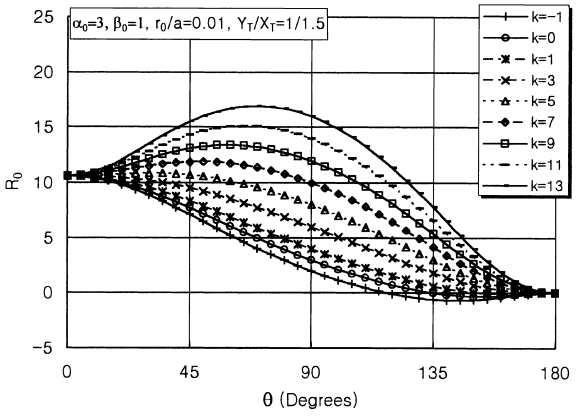

Fig. 8. Variation of R_0 with k for $\alpha_0 = 3$, $\beta_0 = 1$ and $Y_T/X_T = 1/1.5$.

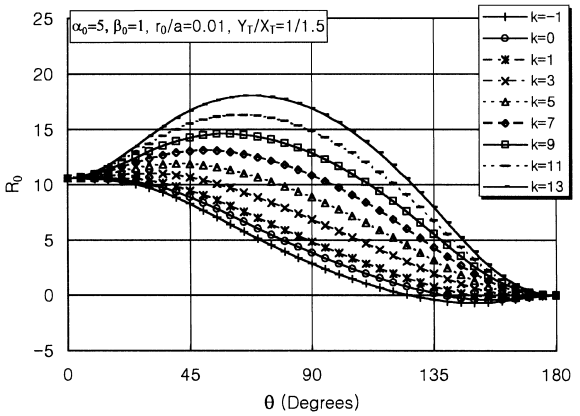

Fig. 9. Variation of R_0 with k for $\alpha_0 = 5$, $\beta_0 = 1$ and $Y_T/X_T = 1/1.5$.

directions of crack extension for singular and subsequent term approximation is given in Table 3. In the table we illustrate the important effects produced by nonsingular terms on the crack growth direction based on the case $r_0/a = 0.01$. Until as elastic modulus ratio $\alpha_0 = 3.0$ the directions predicted by the two approximations are identical to zero. However, it can be seen that the inclusion of the nonsingular term produce markedly different results for the crack propagation direction for the cases considered, particularly as α_0 gets high values. We see that it is possible in the case of a symmetric loaded sheet to have situations where the direction of initial crack extension necessarily deviates from the plane of the original crack.

7. Conclusions

Evidence is accumulating that the predicted crack growth direction may vary with the degree of local in-plane load biaxiality, in addition to its established primary dependence on the elastic stress intensity factor. It is therefore suggested that the prediction of crack extension using only singular term may not be meaningful. The specimen which has been most commonly used for examining crack extension under varying biaxial loading, the central notched plate, is given special attention.

Table 2
Predicted directions of crack extension for various horizontal load ratio with $Y_T/X_T = 1/1.5$ and $\beta_0 = 1.0$

k	θ_0 (degrees)					
	$\alpha_0 = 1/1.2$		$\alpha_0 = 3.0$		$\alpha_0 = 5.0$	
	$r_0/a = 0.01$	: 0.05	$r_0/a = 0.01$	: 0.05	$r_0/a = 0.01$	: 0.05
−1	0	0	0	0	0	0
1	0	0	0	0	±13.6	0
2	0	0	0	0	±23.1	0
3	0	0	0		±29.7	0
4	0	±37.7	±12.2	±34.6	±35.5	±28.2
5	0	±61.3	±32.0	±51.9	±40.9	±40.9
6	0	±69.5	±41.8	±61.7	±45.9	±51.4
7	±20.6	±73.9	±49.0	±67.7	±50.4	±59.5
8	±47.2	±76.8	±54.7	±71.7	±54.5	±65.3
9	±57.0	±78.7	±59.1	±74.5	±58.0	±69.4
10	±62.8	±80.2	±62.6	±76.6	±61.1	±72.4
11	±66.7	±81.3	±65.6	±78.2	±63.7	±74.7
12	±69.6	±82.2	±67.8	±79.4	±65.9	±76.5
13	±71.9	±82.9	±69.8	±80.4	±67.9	±77.9

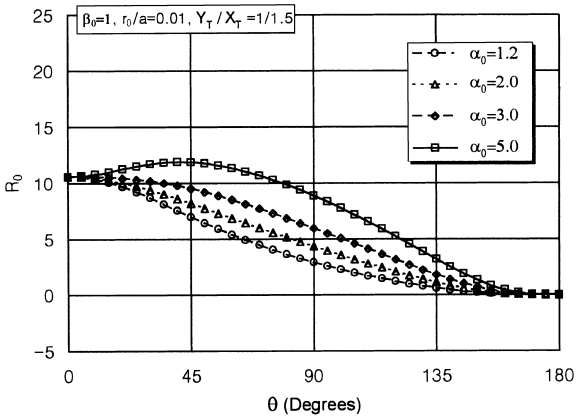

Fig. 10. R_0 for one-term approximation in uniaxially loaded sheet.

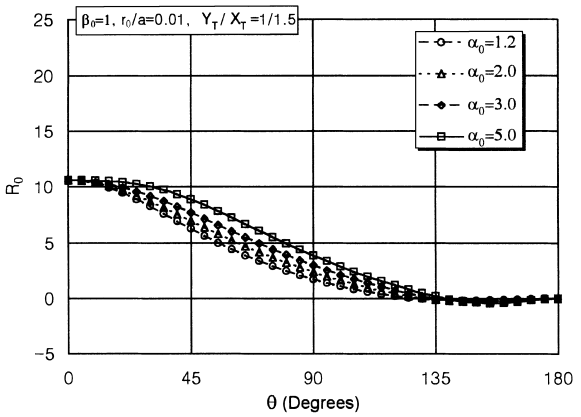

Fig. 11. R_0 for two-term approximation in uniaxially loaded sheet.

Table 3
Predicted directions of crack extension for horizontal crack under uniaxial tension load with $Y_T/X_T = 1/1.5$ and $\beta_0 = 1.0$

α_0	θ_0 (degrees)	
	One-term	Two-term
1.2	0	0
2.0	0	0
3.0	0	0
4.0	31.2	0
5.0	40.9	0

By considering the effect of the load applied parallel to the plane of the crack, the distribution of stresses and displacements at the crack tip has been examined. Present analytical results show significant biaxial loading effects on the crack tip region stresses and displacements, and on the direction of initial crack extension. Inclusion of the nonsingular stress terms along with the normal stress ratio criterion results in significant differences in the predicted direction of crack growth. Thus a detailed experimental study is needed to develop a meaningful criterion for crack branching in orthotropic materials.

References

[1] Sih GC. In: Sih GC, editor. Cracks in materials possessing homogeneous anisotropy in cracks in composite materials. Hague: Martinus Nijhoff, 1981.
[2] Sih GC, Liebowitz H. In: Liebowitz H, editor. Mathematical theories of brittle fracture in fracture mechanics, vol. II. New york: Academic Press; 1968.
[3] Sih GC, Paris PC, Irwin GR. On cracks in rectilinearly anisotropic bodies. Int. J. Fract. 1965;1:189–203.
[4] Buczek MB, Herakovich CT. A normal stress criterion for crack extension direction in orthotropic composite materials. J Compos Mater 1985;19:544–53.
[5] Lekhinitskii SG. Anisotropic plates. New York: Gordon and Breach Science Publishers; 1968.
[6] Savin GN. Stress concentration around holes. Oxford: Pergamon Press; 1961.